FILM BOILING OF DISCRETE DROPLETS OF MIXTURES OF COAL AND WATER ON A HORIZONTAL BRASS SURFACE†

C. T. AVEDISIAN,* C. IOFFREDO‡ and M. J. O'CONNOR§

Sibley School of Mechanical and Aerospace Engineering, Cornell University, Ithaca, NY 14853, U.S.A.

Abstract—The effect of coal on the evaporation of water from mixtures of coal and water was studied in a Leidenfrost-type experiment. Pulverized bituminuous coal was mixed with water in volume concentrations of 14% and 26%, with corresponding total droplet volumes of $0.052 \, cm^3$ and $0.055 \, cm^3$, respectively. Evaporation times were recorded by videotape over a range of plate temperatures from just above the Leidenfrost point of water to 670°K. The test surface used in all the experiments was brass, and the pressure was kept constant at atmospheric.

Three stages in the evaporation lifetime of the coal/water droplets were observed: (1) evaporation of levitated sessile shaped drops; (2) a regime in which physical distortion of the droplet and collapse of the supporting vapor cushion occurred; and (3) a final stage characterized by propagation of a dryout or evaporation front from the bottom of the drop after which a residue of agglomerated coal was left on the surface. This dryout front was used as a measure of the evaporation time of water from the slurry droplet.

Results showed that evaporation times of water were lower in the presence of coal than for a pure water droplet containing the same volume of water as in the corresponding CWM droplet. This was thought to be due mainly to enhancement of heat transfer to the droplet caused by collapse of the vapor film and direct coal/plate contact. An empirical correlation is presented for the total evaporation time of droplets of coal/water mixtures on brass which assumes a linear variation of evaporation time with volume concentration of coal.

1. INTRODUCTION

A promising approach for coal utilization is to mix pulverized coal with a liquid—water or a liquid fuel—and then burn the slurry. This idea is attractive for the following reasons: (1) resources of petroleum based fuels are diminishing so that the substitution of oil by coal or by a mixture of coal and water represents a direct saving of oil; (2) pulverizing and mixing processes are less costly than coal-liquifaction; and (3) the fact that the slurry is fluid-like renders it pumpable so that existing liquid fueled combustors can, in principle, accept the slurry with minimum modification. Of the various types of slurry fuels currently considered as an alternative energy source, coal/water mixtures (CWM) are perhaps the most versatile. They possess an intrinsic combustion potential and are also an effective means of coal transport over large distances. Yet, unlike pure liquid fuels, little is known about the fundamental processes involved in CWM vaporization. The work reported here is a first step toward an understanding of these processes as they relate to CWM droplets on hot surfaces.

The configuration of CWM droplets evaporating on a hot surface is of interest for the following reasons: (1) interaction of fuel droplets with a hot surface is a potentially important evaporation/combustion mode; (2) droplet production is easily controlled and problems of injector clogging due to coal particle agglomeration are minimized; (3) for temperatures above the Leidenfrost point of water, the droplets may be levitated for a portion of their total evaporation time; (4) the effect of suspended particles on the film boiling characteristics of a liquid is essentially unknown and may easily be studied in a Leidenfrost-type experiment; and (5) the droplets are relatively stationary, hence easily photographed.

Previous experimental work on the Leidenfrost phenomenon employed pure liquids, miscible mixtures of liquids, and emulsions over a range of plate temperatures and materials, subcoolings, ambient pressures, and initial droplet volumes[1–9]. Various analytical models have also been presented which are in general agreement with experimental facts[1, 2, 10–14]. The work reported here extends these studies to mixtures of coal and water. The objectives were to (1) measure evaporation times of CWM droplets initially levitated on a hot surface; (2) determine the effect of coal on evaporation of water in a CWM droplet; (3) provide photographic documentation of the various stages of evaporation; and

(4) develop a simple correlation which predicts observed total evaporation times of CWM droplets on a horizontal hot surface. To determine the effects of coal suspensions on evaporation of water droplets, the ambient pressure (0.101 MPa), initial droplet subcooling (75°K), and plate material (brass) were all kept constant. The evaporative behavior of two concentrations of coal in water mixtures were determined − 14% and 26% by volume. The evaporation times of pure water droplets with initial volumes ranging between 0.01 cm³ and 0.05 cm³ were also measured to compare our experimental method with previous work.

2. EXPERIMENT

2.1 *Apparatus*

The principle of our experiment was based on the classic Leidenfrost method in which a droplet is levitated above a hot surface by rapid evaporation of liquid from the bottom of the droplet. In the present work, the test droplets consisted of mixtures of coal and water. Droplets of approximately 50 μl volume were deposited on a dimpled polished horizontal brass surface. Total evaporation times were measured over a range of plate temperatures from 550 to 710°K. The evaporative behavior of the CWM droplets was photographed and recorded on videotape.

A schematic diagram of the apparatus is shown in Fig. 1. The primary components were: (1) a heater block (cylindrical copper billet 6.35 cm in diameter and 8.0 cm long around which two 450 watt band heaters were fastened) with removable polished test surface; (2) the droplet injector (syringe or pipette); (3) a video-optical system and 35 mm camera; and (4) measuring devices such as a digital stopwatch, thermocouples, and a digital voltmeter.

The test surface was a brass disc 6.35 cm in diameter and 1.9 cm thick. A circular area in the center of the surface, 4.45 cm in diameter, was machined as a conical depression 0.76 mm deep. This depression prevented the levitated droplets from sliding off the test surface. The test surface was polished on a lathe to a mirror finish using double-O gauge emery paper and Wenol plus K compound. Subsequent washing by acetone removed any oil residue. The plate was polished in this manner approximately once per every 10 to 15 coal/water droplets to minimize the effects of dirt and coal residue. Brass was chosen as the hot plate material so as to minimize any local surface temperature decrease during film boiling[10, 13].

Surface temperatures were determined by extrapolating the temperature recorded at four locations in the brass disc. Extrapolated surface temperatures were found to be within 0.5°K of the temperature recorded by the uppermost thermocouple. The thermocouples were made from 30 gauge glass braid sheathed chromel–alumel wire. Temperatures were monitored by a digital voltmeter with an ice bath reference. The hot plate temperature was regulated by an Omega temperature controller.

Test droplets were deposited on the plate by hand. Pipettes were used to form the CWM droplets so as to reduce any tendency of clogging. They were discarded after every few CWM droplets. Pure water droplets were formed by a 50 μl calibrated syringe equipped with a flat tipped needle (0.91 mm o.d.).

Various stages in the vaporization history of the CWM droplets were photographically documented by both still photography using a 35 mm camera, and continuously by video tape. Angled front lighting was used for both methods. A coal particle was typically left on the test surface after complete evaporation. This residue was immediately removed by an air jet, with any remaining residue removed by a water jet. Care was taken to ensure a steady plate temperature prior to each experiment. Extraneous heat transfer to the test surface from the lighting used was minimized by heat absorbing glass. Uniform light positions and
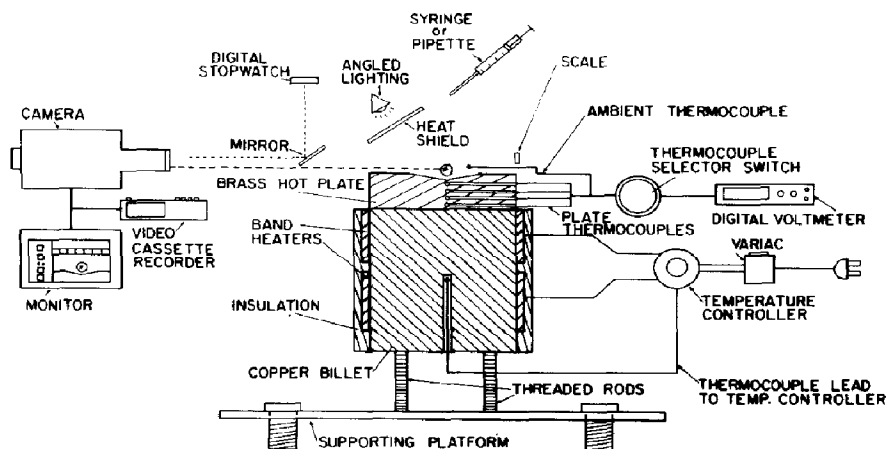

Fig. 1. Schematic diagram of the apparatus.

intensity were maintained throughout our experiments.

Further details of the apparatus and procedures for obtaining the data are described elsewhere[15].

2.2 *Preparation of coal/water mixtures*

A pulverized Pennsylvania bituminous coal (mean particle diameter under 30 μ and $\epsilon \simeq 1.4$) was used in the coal/water mixtures. Coal porosity was measured by packing (tamping) the coal in a graduated cylinder to a pre-selected volume, adding a known volume of water, and then agitating the mixture. The porosity was determined by subtracting the sum of the packed coal volume and water volume from the observed total volume after water addition. An average porosity of about 20% was obtained by this method. This value is dependent on the method of packing so that care was taken to ensure a uniform packing procedure for all mixtures. The porosity was used to prepare the volumes of coal and water required to give a desired CWM.

Dispersal of the coal suspension was affected by an ultrasonic transducer at 20,000 Hz using a Fisher sonic dismembrator. The mixture was continuously agitated in this way throughout an experiment because of the poor stability of the CWM. The addition of surfactants to the water (Tween 80 and 85) was found to have no discernable effect on CWM stability.

The process of withdrawing a CWM sample from the mixing beaker and transferring a droplet to the hot plate created some uncertainty about the actual volume of coal in the test droplets. Ths suspension tended to settle in the pipette during transfer from the agitated beaker to the hot plate. It was found that the average coal concentration was larger in the transferred sample than in the continuously agitated mixture[15]. For the two coal/water mixtures prepared—10 and 20%—the actual volume percent of coal in the test droplets was measured to be 14 and 26% respectively.

3. DISCUSSION
3.1 *Experimental observations*

Preliminary experiments were performed to ascertain the variation of evaporation time with plate temperature and the effect of initial droplet volume on evaporation time of pure water droplets in the levitated state. These results were compared to those of previous studies to delineate boundaries for the onset of film boiling as a lower limit on plate temperature for the levitated state of the CWM droplets tested.

Figure 2 illustrates a complete evaporation time curve for water droplets of 0.01 cm³ volume on brass. The data plotted correspond to the time of complete disappearance of the liquid after initial deposition on the test surface. A definite Leidenfrost point, T_{Leid}, for pure water droplets was observed. This point was taken to correspond to the maximum evaporation time of droplets in film boiling[13]. The observed temperature of about 526°K (Fig. 2) is, within experimental error, in agreement with previous work[7,16]. At higher temperatures the droplets were levitated by a vapor cushion and were observed initially to oscillate rapidly. At lower temperatures (between 526 and 400°K) unstable or transition boiling was observed, characterized by intermittent solid/liquid contact and periodic collapse of the vapor film. Repeatable measurements were difficult to obtain in this temperature range. Below 400°K the droplets wetted the surface on impact and quietly evaporated.

Figure 3 illustrates the effect of initial droplet volume on evaporation time for pure water droplets when $T_p > T_{Leid}$. The general trends shown are consistent with the expectation that larger droplets take longer to evaporate completely. Results from Emmerson's[7] study of water droplets on brass are also
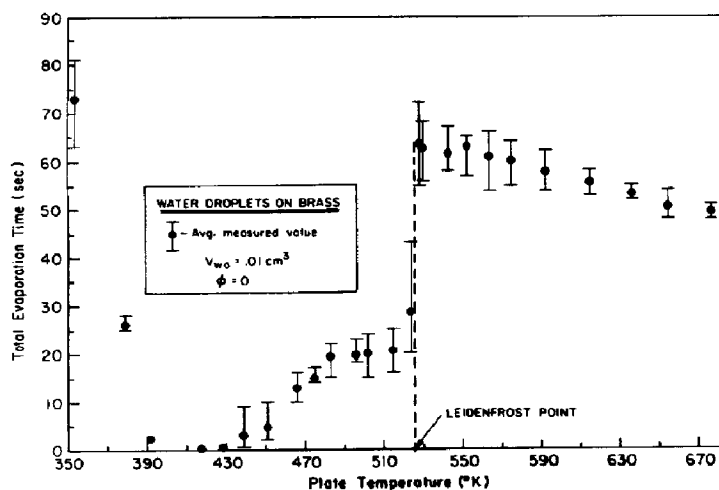
Fig. 2. Complete evaporation time curve for pure water on brass ($V_{w0} = 0.01$ cm³).
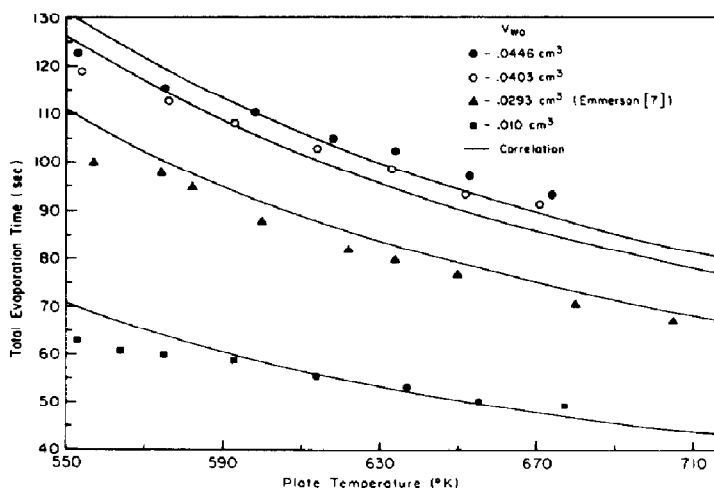
Fig. 3. Variation of vaporization time with plate temperature for pure water droplets of various initial volumes (V_{wo}) for droplets initially levitated ($T_p > T_{Leid}$).

included to illustrate the consistency of the present measurements.

Three stages of evaporation of initially levitated CWM droplets were consistently observed for $T_p > T_{Leid}$. Figure 4 shows a photographic sequence of these stages. The first stage was characterized by a period of levitation above the test surface (Fig. 4a). The droplet, supersaturated with water, was sessile in shape with a relatively flat base. These droplets were observed to spin occasionally, but no oscillations such as were evident in pure water droplets containing the same volume of water as in the corresponding CWM were observed. In the second or intermediate stage (Fig. 4b) the water content decreased to an extent where physical distortion of the droplets occurred. This was evidenced by a "wrinkling" of the droplet surface. During this stage the vapor cushion apparently collapsed as evidenced by an abrupt cessation of spinning and any fluid like motion of the
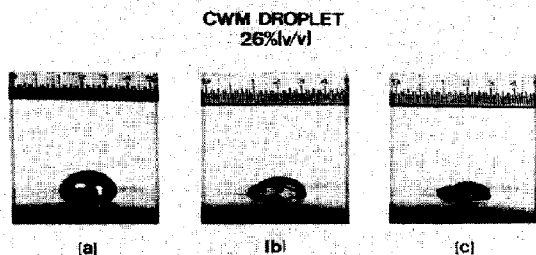

Fig. 4. Photographic sequence of a 26% (v/v) coal/water mixture droplet evaporating on a brass surface. $V_{wo} \simeq 0.05 \text{ cm}^3$, $T_p \simeq 573°\text{K}$. Scale marked in intervals of 0.25 mm (a) initial levitation of the droplet; (b) wrinkling and distortion of droplet surface; (c) collapse of vapor cushion and propagation of evaporation front (interface between light and dark areas). Evaporation front used as measure of total water evaporation time.

droplet. The final stage of evaporation was characterized by propagation of a dryout or evaporation front from the bottom to the top of the droplet (Fig. 4c). Disappearance of this front was taken to signify the final evaporation of water, after which a residue of agglomerated coal was left on the surface. Continued heating of this residue would presumably result in its eventual ignition, but this was never observed for the range of plate temperatures we studied.

Collapse of the vapor film could have been due to an inability of water to pass through an essentially porous medium inside the droplet at a rate sufficient to replenish the mass lost by vaporization at the base of the droplet, but this is just conjecture. In coal/water mixtures a resistance to flow could be created by a "choking" or "blocking" effect caused, perhaps, by sedimentation of coal at the base of the droplet. Dryout at the base would then occur and the droplet would impact the surface. (Oscillations of CWM droplets were not observed, so that the mechanism for vapor film collapse suggested by Hall[17] for pure liquids will not apply to CWM droplets.)

The effect of coal addition to a fixed volume of water, V_{wo}, on the total liquid phase evaporation time is shown in Figs. 5 and 6. Also shown are the evaporation times of pure water droplets containing the same amount of water (V_{wo}) as in the CWM droplets studied. (Thus, the CWM droplets had a larger overall volume than the corresponding water droplets of volume V_{wo} by the factor $1/(1 - \phi)$). The CWM evaporation times shown in these two figures represent the total time from initial deposition to disappearance of the evaporation front (Fig. 4c). Individual CWM evaporation times are plotted without any averaging. The pure water data are an average of at least ten measurements.

Difficulties with rapid surface contamination after vapor film collapse precluded studying more than five
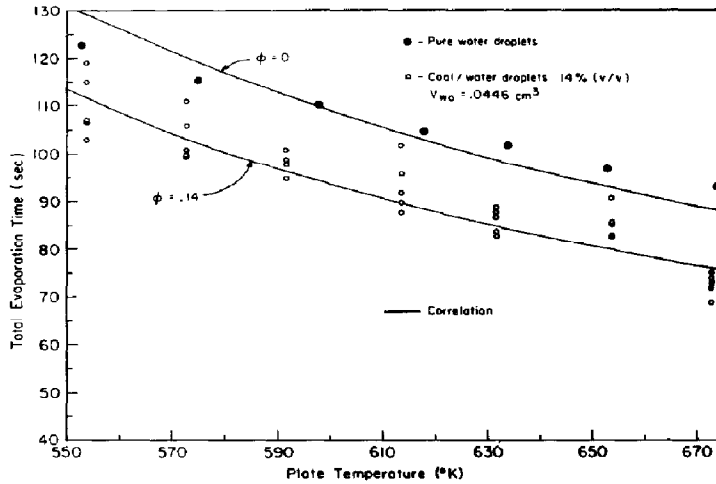
Fig. 5. Variation of evaporation time with plate temperature for 14% (v/v) coal/water mixture droplets with $V_{w0} \simeq 0.045\,\mathrm{cm}^3$. $\bigcirc$, 14% CWM; $\bullet$, pure pater droplets with initial volume of about $0.045\,\mathrm{cm}^3$.
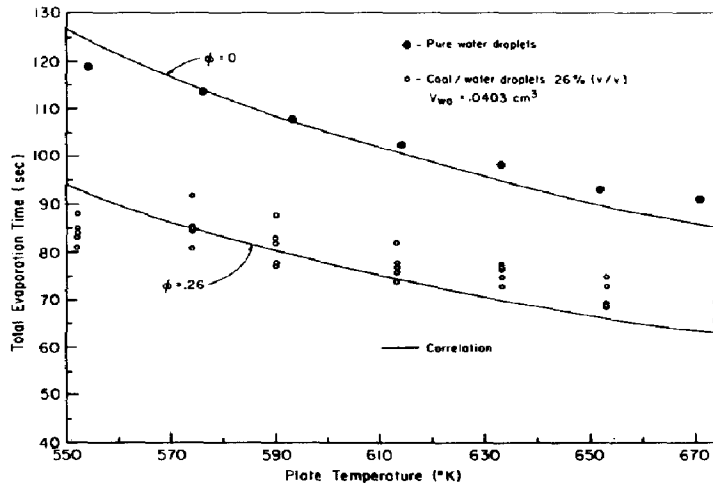
Fig. 6. Variation of evaporation time with plate temperature for 26% (v/v) coal/water mixture droplets with $V_{w0} \simeq 0.04\,\mathrm{cm}^3$. $\bigcirc$, 26% CWM; $\bullet$, pure water droplets with initial volume of about $0.04\,\mathrm{cm}^3$.

CWM droplets at a given plate temperature before the surface had to be repolished. This problem was most pronounced when $T_p < T_{\mathrm{Leid}}$. In this temperature range, the CWM droplets were not initially levitated, but rather direct coal/plate contact occurred. Intermittent splattering of coal over the brass surface effected the evaporative behavior of subsequently deposited droplets thus making it difficult to unambiguously measure evaporation time. For this reason only data for CWM droplets initially in film boiling ($T_p > T_{\mathrm{Leid}}$) were made. For these measurements, the brass surface was polished to a mirror finish after each series of droplets were studied at each plate temperature. Evaporation times of the first droplets deposited on the freshly polished surface showed no systematic variation compared to the last droplet studied at a given plate temperature.

Figures 5 and 6 show that liquid phase evaporation times are lower for water in a CWM containing a volume V_{w0} of water than for a pure water droplet of the same volume V_{w0}. A mechanism conjectured to be responsible for this effect is an increase in heat transfer to the droplet due to the weight of the coal. A simple model for this effect is presented in the next section. Because of the nature of the approximations involved in the model, the results are quantitatively used only as a basis for correlating our experimental results.

3.2 *Correlation for evaporation time*

The primary mechanism for evaporation of a droplet in film boiling on a hot surface is heat transfer and vaporization at the base of the droplet. A flow of vapor is thereby created underneath the droplet. The corresponding pressure gradient provides the force that levitates the droplet above the surface. We use basic conservation laws to develop a simple expression for CWM droplet evaporation time based on the above ideas. We do not explicitly address the complicated problem of vapor film collapse, but rather assume the CWM droplets remain levitated throughout their evaporative lifetime. (This assumption will strictly apply only in the limit of a dilute CWM wherein $\phi \to 0$. In this limit there is a negligible difference in time between vapor film collapse and propagation and disappearance of the evaporation front.) Evaporation over the upper surface of the CWM droplets due to molecular diffusion is also neglected. This is a good approximation as previous correlations neglecting molecular diffusion[1, 11, 14] have been in nearly as good agreement with data as correlations which have included this effect[1, 14]. The neglect of this effect for CWM droplets is convenient due to a lack of data on diffusion coefficients of liquids from the free surface of slurries.

The model of an evaporating CWM droplet in film boiling is shown in Fig. 7. The base of the droplet is assumed to be planar out to a radius R_0 where the pressure is atmospheric. Evaporation at the droplet base creates a vapor outflow resembling flow in a channel. Following previous work for pure liquids[1, 2, 14] we assume a fully developed laminar vapor flow with no-slip conditions applying at the CWM/vapor interface and hot plate. The corresponding parabolic velocity profile together with a simple mass balance in the vapor film gives the pressure distribution in the film in terms of the vertical vapor velocity, v_0, as

$$P(x) - P_0 = \frac{3\mu_g v_0}{\delta^3}[R_0^2 - x^2]. \tag{1}$$

This pressure distribution produces an upward force at the base of the droplet which is counterbalanced by the weight of the droplet. From a force balance we have that (gravity vector is normal to the test surface)

$$\int_0^{R_0} (P - P_0)2\pi x \, dx = \rho_w g V_{w0}\left[\bar{V}_w + \frac{\phi}{1-\phi}\epsilon\right]. \tag{2}$$

Combining eqns (1) and (2) and integrating, we obtain a relation between the vapor film thickness, δ, and v_0 as

$$\delta = \left[\frac{3}{2}\frac{v_0\mu_g\pi R_0^4}{V_{w0}\rho_w g\left(\frac{\phi}{1-\phi}\epsilon + \bar{V}_w\right)}\right]^{1/3}. \tag{3}$$

Except for the term in ϕ and ϵ in the denominator, eqn (3) is similar to previous results[1, 2, 11, 14].

A heat balance at the base of the droplet equates the energy absorbed by vaporization to heat conducted across the vapor film. For pure liquids, $\delta \sim 0.003$ cm[18] and we do not expect this value to be appreciably different for CWM droplets. It is, therefore, reasonable to assume a linear temperature distribution across the vapor film (Fig. 7b). For the range of plate temperatures we studied the contribution to the total heat transfer by radiation was found to be negligible, compared to heat conduction across the vapor film. Similarly, radiation to the sides of the droplet from the plate was also estimated to be negligible. The vertical vapor velocity may then be written as

$$v_0 \simeq \frac{k_g \Delta T}{\rho_g h_{fg}\delta}. \tag{4}$$

Finally, an overall energy balance yields

$$h_{fg}\rho_w V_{w0}\frac{d\bar{V}_w}{dt} = -A_b k_g \frac{\Delta T}{\delta}. \tag{5}$$

Combining eqns (3)–(5) and integrating gives

$$t = \xi \frac{V_{w0}^{5/12}}{\Delta T^{3/4}} \cdot I(\phi, \epsilon, \bar{V}_w) \tag{6}$$

ξ is a function of physical properties (which we take to be essentially constant) and I represents an integral of the conservation equations. Eqn. (6) displays the same general dependence of t on V_{w0} and ΔT reported by others (e.g. [1, 11, 14]). An explicit expression for I depends on droplet shape. Assuming the droplet to be in the shape of a truncated oblate spheroid, I takes on the approximate form (Appen-
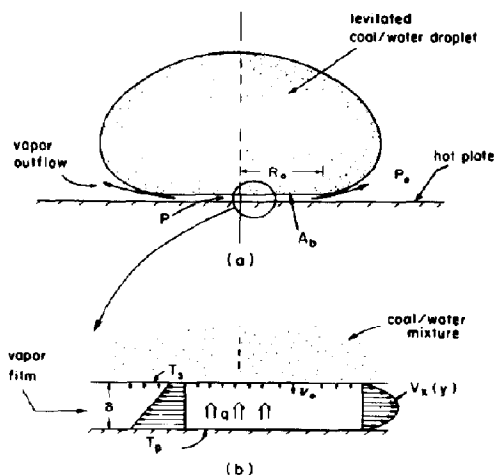

Fig. 7. Schematic illustration of a levitated coal/water mixture droplet.

dix 1)

$$I \simeq \frac{12}{5}\left\{(1-\phi)^{-5/12} - \left(\frac{\phi}{1-\phi} + \bar{V}_w\right)^{5/12}\right\}$$

$$+ \frac{3}{7}(\epsilon - 1)\frac{\phi}{1-\phi}\left\{(1-\phi)^{7/12}\right. \tag{7}$$

$$\left. - \left(\frac{\phi}{1-\phi} + \bar{V}_w\right)^{-7/12}\right\}.$$

When $\bar{V}_w \to 0$, $t \to t_e$ and eqs (6) and (7) become, in principle, an expression for the total liquid phase evaporation time. However, for $\phi > 0$ these equations are not applicable for two reasons: (1) the droplets do not remain levitated throughout their evaporative lifetime (Fig. 4c); and (2) the droplet shape becomes distorted and its structure collapses into an ill defined shape (Fig. 4b). As a result, we used eqns (6) and (7) only as a basis for correlating our experimental results. In this regard, we note that in the limit when $\phi \to 0$, the assumed model more closely represents physical reality. In this limit, there is a negligible difference in time between the onset of distortion of the initially spheroidal droplet shape, vapor film collapse, and propagation and disappearance of the evaporation front.

In the limit when $\bar{V}_w = 0$ and $\phi \to 0$ eqns (6) and (7) may be combined to yield

$$t_e \simeq C_1 \frac{V_{w0}^{5/12}}{\Delta T^{3/4}}(1 - C_2\phi^{C_3}) \tag{8}$$

where, from the present model, $C_1 = 12/5\xi$, $C_2 = \{1 + 5/28(\epsilon - 1)\}$, and $C_3 = 5/12$. The basis of our empirical correlation was to consider C_1, C_2 and C_3 adjustable constants whose values were selected to give optimum agreement with our measurements. C_1 was determined from pure water ($\phi = 0$) evaporation time data (which were taken under the same ambient gas, surface material, and surface finish conditions as our CWM data). $C_1 \simeq 7.398 \times 10^6 \, °K^{3/4} - s/cm^{5/4}$ was found to represent all of our pure water data quite well as shown in Fig. 3 (units of V_{w0} and ΔT are m^3 and °K respectively). For the coal/water mixtures studied, $C_2 - C_3 = 1$ was found to work best.

Figures 5 and 6 illustrate a comparison between measured evaporation times and values of t_e calculated from eqn (8) for 14% and 26% CWM droplets, respectively. The agreement shown serves as an indication of the usefulness of the present empirical correlation for predicting the effect of coal volume concentration and plate temperature on evaporation time of CWM droplets initially in film boiling ($T_p > T_{Leid}$) on a *horizontal* surface.

The use of eqn (8) to predict evaporation times of CWM droplets in film boiling on a hot horizontal surface even when direct plate/droplet contact may occur during evaporation is an attempt, in a simple way, to provide a useful formulation for predicting

evaporation times of water in a CWM. The success of the method is evidenced by the results shown in Figs. 5 and 6 for the data reported herein. More rigorous approaches should take into account the actual droplet shape and the effect of vapor film collapse.

4. CONCLUSIONS

Evaporation characteristics of droplets of coal/water mixtures initially in film boiling on a hot surface were studied. The effect of coal addition to a given volume of water was two-fold: (1) to lower the total evaporation time of water, and (2) to bring about destruction of the vapor film on which the droplets were initially levitated. This latter effect is unique to CWM droplet evaporation on a surface above the Leidenfrost point of water.

A simple physical model based on evaporation at the bottom of the droplet was used to correlate our measurements. The model assumed the levitated state was maintained throughout the droplet lifetime. The results were in good agreement with our pure water data. CWM evaporation times were well correlated by assuming a linear relation between evaporation time and volume concentration of coal.

NOTATION

A_b flat evaporation area at base of levitated droplet, πR_0^2
C empirical constant (eqn 8)
g gravitational acceleration
h_{fg} heat of vaporization of water
k_g thermal conductivity of the vapor film
P_0 ambient pressure surrounding the droplet
$P(x)$ pressure in vapor film at x
R_0 radius at base of the droplet where $P(x) = P_0$
t_e evaporation time
T_{Leid} Leidenfrost temperature of water
T_p surface temperature of the hot plate
T_s droplet temperature (373°K at 0.101 MPa)
V_w volume of water in a CWM
V_{w0} initial volume of water in a CWM
$\bar{V}_w$ nondimensional water volume, V_w/V_{w0}
x radial position from droplet center, $0 < x < R_0$

Greek symbols
δ thickness of the vapor film
ΔT $T_p - T_s$
ϵ coal to water density ratio, ρ_c/ρ_w
ϕ initial volume fraction of coal in a CWM
ρ_g density of the vapor film
ρ_w water density

μ_g vapor viscosity in film beneath levitated droplet

v_0 vertical evaporation velocity at the base of the droplet

REFERENCES

[1] Gottfried B. S., Lee C. J. and Bell K. J., *Int. J. Heat Mass Transfer* 1966 **9** 1167.

[2] Wachters L. H. J., Bonne H. and von Nouhuis H. J., *Chem. Engng Sci.* 1966 **21** 923.

[3] Bell K. J., *Chem. Engng Prog. Symp. Ser.* 1967 **63**(79) 73.

[4] Godleski E. S. and Bell K. J., *Proc. 3rd Int. Heat Transfer Conf.* Vol. 4, pp. 51–58. Chicago 1966.

[5] Sheffield S. A., Baer M. R. and Denison G. J., *Fall Technical Meeting, The Eastern Section of the Combustion Institute,* paper No. 42. Princeton, 12–14 November 1980.

[6] Baer M. R., Sheffield S. A. and Denison G. J., *Fall Technical Meeting, The Eastern Section of the Combustion Institute,* paper No. 43. Princeton, 12–14 November 1980.

[7] Emmerson G. S., *Int. J. Heat Mass Transfer* 1975 **18** 381.

[8] Emmerson G. S. and Snoek C. W., *Int. J. Heat Mass Transfer* 1978 **21** 1081.

[9] Temple-Pediani R. W., *Proc. Inst. Mech. Engrs* 1969–70 **184**(38) 677.

[10] Baumeister K. J. and Simon F. F., *ASME J. Heat Transfer* 1973 **95**(2) 166.

[11] Baumeister K. J., Hamill T. D. and Schoessow G. J., *Proc. 3rd Int. Heat Transfer Conf.* Vol. 4, pp. 66–73. Chicago 1966.

[12] Rhodes T. R. and Bell K. J., *Proc. 6th Int. Heat Transfer Conf.* Vol. 1, pp. 251–255. Toronto 1978.

[13] Nishio S. and Hirata M., *Proc. 6th Int. Heat Transfer Conf.,* Vol. 1, pp. 245–250. Toronto 1978.

[14] Gottfried B. S. and Bell K. J., *Ind. Engng Chem. Fundls* 1966 **5**(4) 561.

[15] Ioffredo C. and O'Connor M. J., M. Eng. Project Report, Dept. of Mech. and Aero. Engng, Cornell University, Ithaca, New York 1982.

[16] Borishansky V. M., in *Problems of Heat Transfer during a Change of State: a Collection of Articles,* 1953, AEC-TR-3405.

[17] Hall W. B., *Proc. 5th Int. Heat Transfer Conf.* Vol. 4, pp. 125–129. Tokyo 1974.

[18] Kistemaker J., *Physica* 1963 **29** 96.

APPENDIX 1

An approximate analytical integration of eqn (5) may be obtained by assuming the initially levitated droplet to be in the shape of a truncated oblate spheroid (see Fig. A1). This shape closely approximates the actual initial sessile configuration. If the ratio of major to minor axis is α, and Φ (Fig. A1) is the factor by which the minor axis is truncated, then the droplet volume V and base heat transfer area A_b (flat) are given by the following expressions:

$$V = \frac{4}{3}\pi R^3 f_1 \tag{A1}$$

and

$$A_b = \pi R_0^2 \tag{A2}$$

where

$$f_1 = \alpha^2\left[\Phi^3 + \frac{3}{2}\left\{\frac{1}{3}(1-\Phi^2)^{3/2} - \frac{\Phi}{2}(1-\Phi^2)\right\}\right], \tag{A3}$$

$$R_0 = R f_2^{1/2}, \tag{A4}$$

$$f_2 = \alpha^2(1-\Phi^2) \tag{A5}$$

Also, by definition

$$V = V_{w0}\left(\frac{\phi}{1-\phi} + \mathcal{V}_w\right). \tag{A6}$$

Combining eqns (A1)–(A6) and eqn (3) gives

$$A_b = \pi\left(\frac{3}{4\pi f_1}\right)^{2/3} f_2 V_{w0}^{2/3}\left(\frac{\phi}{1-\phi} + \mathcal{V}_w\right)^{-2/3} \tag{A7}$$

and

$$\delta = \left[\frac{3}{2}\frac{\mu_g \pi k_g \Delta T}{V_{w0}\rho_w \rho_g h_{fg} g}\right]^{1/4}\left(\frac{3}{4\pi f_1}\right)^{1/3} f_2^{1/2} V_{w0}^{1/3}\frac{\left[\frac{\phi}{1-\phi} + \mathcal{V}_w\right]^{1/3}}{\left[\frac{\phi}{1-\phi}\epsilon + \mathcal{V}_w\right]^{1/4}} \tag{A8}$$

From eqn (A7) it is seen that for $\phi > 0$ the base area is larger than the base area corresponding to $\phi = 0$ (for the same initial water volume V_{w0}). Equation (A8) shows that the film thickness decreases when $\epsilon > 1$ (which is the case for coal) compared to the film thickness which would exist for a neutrally buoyant ($\epsilon = 1$) inert solid; the opposite is true when $\epsilon < 1$. The combined effect of these two results is that heat transfer to the droplet is increased in the presence of coal (or any inert substance for $\epsilon > 1$), thereby increasing the liquid phase evaporation rate and reducing the total evaporation time, compared to the evaporation time in the absence of coal ($\phi = 0$). This result is in general qualitative agreement with experimental observation.

Upon substituting eqns (A7) and (A8) into eqn (5), assuming α and Φ are independent of time, and integrating
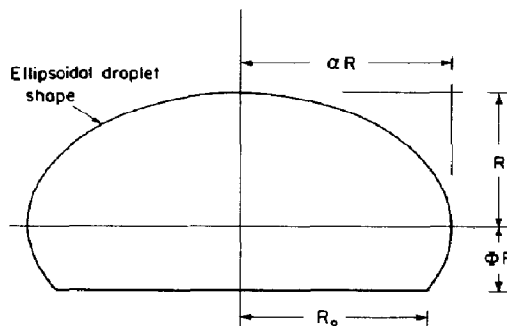

Fig. A1.

gives eqn (6) with

$$\xi = \left[\frac{2^{5/3}}{3^{1/3}\pi^{5/3}} \frac{\mu_g h_{fg}^3 \rho_w^3}{g\rho_g k_g^3}\right]^{1/4} \frac{f_1^{1/3}}{f_2^{1/2}}, \qquad \text{(A9)}$$

and

$$I = \int_0^{\bar{V}_w} g(\bar{V}_w)\, d\bar{V}_w, \qquad \text{(A10)}$$

where

$$g(\bar{V}_w) = \left(\frac{\phi}{1-\phi} + \bar{V}_w\right)^{-1/3} \cdot \left(\frac{\phi}{1-\phi}\epsilon + \bar{V}_w\right)^{-1/4}. \qquad \text{(A11)}$$

An approximate evaluation of I can be obtained by linearizing g with respect to ϵ about $\epsilon = 1$. Doing so and integrating yields

$$I \simeq \frac{12}{5}\left\{(1-\phi)^{-5/12} - \left(\frac{\phi}{1-\phi} + \bar{V}_w\right)^{5/12}\right\} \qquad \text{(A13)}$$

$$+ \frac{3}{7}(\epsilon - 1)\frac{\phi}{1-\phi}\left\{(1-\phi)^{7/12} - \left(\frac{\phi}{1-\phi} + \bar{V}_w\right)^{-7/12}\right\}$$

which is eqn (7). Equation (A13) is an excellent approximation to an "exact" evaluation of eqn (A10) for $1 < \epsilon < 1.5$ as shown via numerical integration of eqn (A10).